
HIERARCHY-GUIDED MODEL SELECTION FOR TIME SERIES FORECASTING

A PREPRINT

Arindam Jati
IBM Research
Bangalore, India
arindam.jati@ibm.com

Vijay Ekambaram
IBM Research
Bangalore, India
vijayel2@in.ibm.com

Shaonli Pal*
IIT Jodhpur
Jodhpur, India
palshaonli1234@gmail.com

Brian Quanz
IBM Research
Yorktown Heights, NY, USA
blquanz@us.ibm.com

Wesley M. Gifford
IBM Research
Yorktown Heights, NY, USA
wmgifford@us.ibm.com

Pavithra Harsha
IBM Research
Yorktown Heights, NY, USA
pharsha@us.ibm.com

Stuart Siegel
IBM Research
Yorktown Heights, NY, USA
stus@us.ibm.com

Sumanta Mukherjee
IBM Research
Bangalore, India
sumanm03@in.ibm.com

Chandra Narayanaswami
IBM Research
Yorktown Heights, NY, USA
chandras@us.ibm.com

November 29, 2022

ABSTRACT

Generalizability of time series forecasting models depends on the quality of model selection. Temporal cross validation (TCV) is a standard technique to perform model selection in forecasting tasks. TCV sequentially partitions the training time series into train and validation windows, and performs hyperparameter optimization (HPO) of the forecast model to select the model with the best validation performance. Model selection with TCV often leads to poor *test* performance when the test data distribution differs from that of the validation data. We propose a novel model selection method, `H-PRO` that exploits the data hierarchy often associated with a time series dataset. Generally, the aggregated data at the higher levels of the hierarchy show better predictability and more consistency compared to the bottom-level data which is more sparse and (sometimes) intermittent. `H-PRO` performs the HPO of the lowest-level student model based on the *test proxy forecasts* obtained from a set of teacher models at higher levels in the hierarchy. The consistency of the teachers' proxy forecasts help select better student models at the lowest-level. We perform extensive empirical studies on multiple datasets to validate the efficacy of the proposed method. `H-PRO` along with off-the-shelf forecasting models outperform existing state-of-the-art forecasting methods including the winning models of the M5 point-forecasting competition.

1 Introduction

Time series data is often associated with a hierarchy. For example, in the retail domain, daily sales of a certain product in a store constitute a product-level time series. Aggregating all product-level time series in the store at each time point gives a cumulative store-level series consisting of the daily sales of that particular store. Similarly, aggregated time series can be obtained at other levels like department, state, and country Makridakis et al. [2022]. The notion of generating forecasts at every level of the data hierarchy is generally termed as “hierarchical time series forecasting” Hyndman and Athanasopoulos [2021], and it has been an active area of research in recent years (see Section 3). Hierarchical

*The author was in IBM Research while the work was done.

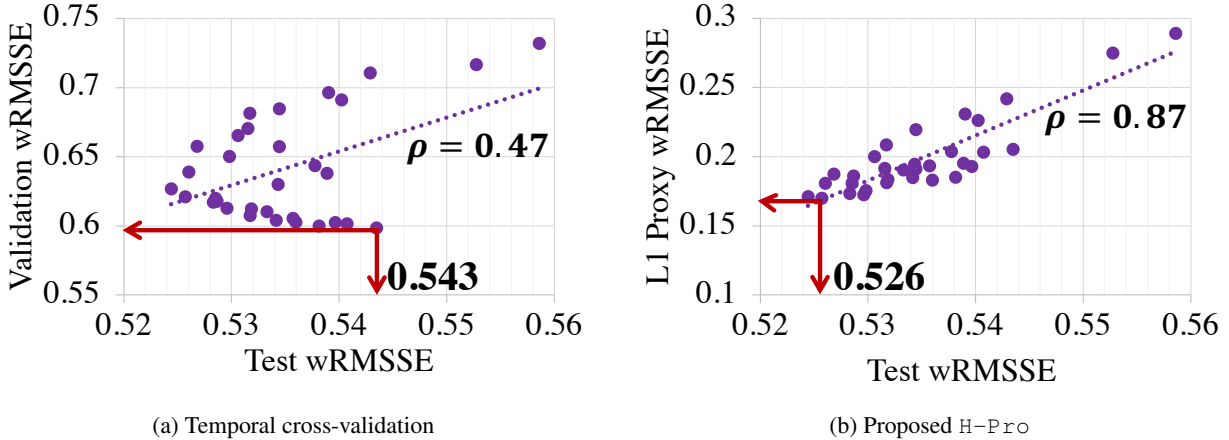


Figure 1: Variation of test error with (a) validation, and (b) proxy errors in all HPO trials (*dots*) for a store-clustered LightGBM model on M5 data. (a): Lowest validation errors do *not* correspond to the lower range of test errors due to data mismatch. (b): The lowest proxy error often selects a model with better test error, and better linear fit is observed with higher correlation, ρ , between test and proxy errors.

forecasting generally requires *coherent* forecasts at every level; i.e., the forecast at an aggregated level should be the exact sum of the forecasts of its children nodes in an associated hierarchy tree. Accurate and coherent forecasts at different levels of the hierarchy ensure that consistent and correct business decisions are taken at different parts of an organization.

A hierarchical forecasting algorithm consists of two components (either decoupled or integrated): a base-forecasting method, and a reconciliation technique that ensures coherent forecasts. Recently, complex machine learning (ML) models with a large number of hyperparameters are becoming popular in forecasting since they can learn from multiple time series and leverage the shared information between them, contrary to some of the classical forecasters like SARIMA, exponential smoothing, *etc.* Examples include gradient boosting models like LightGBM Makridakis et al. [2022], and DNN-based models like DeepAR Salinas et al. [2020], N-BEATS Oreshkin et al. [2020], and Informer Zhou et al. [2021]. This leads to an increase in the adoption of complex ML models for hierarchical forecasting as well due to their superior performance Rangapuram et al. [2021], Paria et al. [2021], Das et al. [2022], Mancuso et al. [2021].

The performance of these models depends on hyperparameters that are generally tuned on validation window(s) via temporal cross-validation (TCV) Hyndman and Athanasopoulos [2021]. TCV chronologically splits the historical time series data into train and validation windows. Thus, the validation windows often differ in characteristics from the test data. The mismatch between validation and test is prevalent in time series compared to other ML domains because of varying statistical properties of temporal data Hyndman and Athanasopoulos [2021], Akgiray [1989]. The problem is exacerbated in hierarchical forecasting because of higher data irregularity (and sometimes intermittency) at the lowest level. This can lead to suboptimal hyperparameter optimization (HPO) and poor model selection, particularly at the lowest level of the hierarchy (see Figure 1(a)).

We propose a novel HPO technique for hierarchical time series forecasting. It is based on the frequent observation that time series at the lowest level of the hierarchy are sparse, irregular, and sometimes intermittent in nature such as in Makridakis et al. [2022]. However, the aggregated series at higher levels are generally more consistent and have better predictability. Based on this observation, we develop $H-PRO$, a method for performing HPO of the lowest-level forecasting model based on one or more *proxy forecaster(s)* at higher levels. The proxy forecasters are trained on higher-level aggregated time series, and their forecasts for the *test* period are obtained. The lowest-level model treats these forecasts as proxies to the original time series for the test period, and the HPO of the lowest-level model is performed with respect to the higher-level proxy forecasts instead of validation windows as done in conventional TCV (Figure. 2). Thus, by effectively leveraging the better predictability of the aggregated series, the lowest-level models are regularized via HPO. The lowest-level forecasts are then aggregated bottom-up (Section 3) to derive higher-level forecasts leading to coherent and accurate forecasts at all levels. From Figure 1(b), we can see that $H-PRO$ helps in model selection, i.e., choosing a model with the minimum proxy error criteria corresponds to a much better test error compared to conventional TCV.

Summary of contributions

(1) To address the commonly occurring test-validation mismatch issue in forecasting, we propose a novel technique, `H-PRO` that drives HPO via test proxies by exploiting the data hierarchy and better predictability of higher level forecasters. (2) To the best of our knowledge, this is the first work which empirically and theoretically demonstrate that we can obtain coherent and accurate hierarchical forecasts just by employing hierarchical proxy-guided HPO on off-the-shelf ML models. Specifically, `H-PRO` outperforms state-of-the-art results on `Tourism`, `Tourism-L`, `Traffic`, and `Wiki` data, and even the winning method results of the M5 accuracy competition. (3) State-of-the-art hierarchical reconciliation methods like `MinT` and `ERM` (Section 3) can be computationally expensive for datasets with large number of time series, but the proposed `H-PRO` does not suffer from this scalability issue. A detailed comparison is in Appendix A. (4) We also show in experiments that `H-PRO` helps improve the performance of `TCV` when ensembled with it, and hence, emphasize the complementary knowledge captured by the method.

2 Background and Notations

2.1 Forecasting

Let $x_{1:T}$ represent a univariate time series of length T , i.e., at any time-point t , $x_t \in \mathbb{R}$. The task of forecasting is to predict H value(s) in the future given the history $x_{1:T}$,

$$\hat{x}_{T+1:T+H} = f(x_{1:T}) \quad (1)$$

where $f(\cdot)$ is the map learned by a forecasting algorithm \mathcal{A} , and H is the forecast horizon. Here we focus on algorithms that learn a shared map f for multiple related time series, as these often work best in practice (e.g., modern forecasting models like DeepAR, N-BEATS, and LightGBM).

2.2 Hierarchical forecasting

A hierarchical time series dataset is associated with a hierarchy tree that has L levels ($l = 1$ for the top level, and $l = L$ for the lowest level). We denote the set of levels by $[L] = \{1, \dots, L\}$, and the nodes at a level l by $[N_l] = \{1, \dots, N_l\}$. The time series at the leaf nodes are called *lowest-level* series, and the time series at other nodes are called *higher-level/aggregated* series. The higher-level series at any node $j \in [N_l]$ of level $l \in [L - 1]$ follows the coherence criteria Hyndman and Athanasopoulos [2021]: $x_t^{l,j} = \sum_{i \in C_{l,j}} x_t^{(l+1),i}$, where $C_{l,j}$ is the set of children of node j of level l . The task is to forecast accurately at all nodes of all levels so that the forecast at any higher-level node also follows the coherence constraint, i.e., $\hat{x}_t^{l,j} = \sum_{i \in C_{l,j}} \hat{x}_t^{(l+1),i}$, $\forall l \in [L - 1], j \in [N_l]$.

Hierarchical evaluation

Hierarchical forecasts are evaluated with a hierarchically aggregated metric that can indicate the average error across all levels Makridakis et al. [2022]. Generally, every level is given equal weight while aggregating the level-wise metrics, ensuring unbiased evaluation of hierarchical forecasts across all levels. Hence, any hierarchical forecasting technique should aim to attain accurate and coherent forecasting at all levels. More details will be provided in Section 5.

3 Related work

Classical methods of hierarchical forecasting rely on generating base forecasts for every time series, and reconcile them to produce coherent forecasts at every level. For example, the bottom-up (BU) approach produces lowest level forecasts, and simply aggregates them to obtain coherent forecasts at all levels Hyndman and Athanasopoulos [2021]. Similarly, top-down and middle-out approaches take particular aggregate level forecasts and disaggregate them to lower levels Hyndman and Athanasopoulos [2021]. The `MinT` algorithm takes independent forecasts and produces coherent hierarchical forecasts by incorporating information from all levels simultaneously via a linear mapping to the base series Wickramasuriya et al. [2019]. `MinT` minimizes the sum of variances of the forecast errors when the individual forecasts are unbiased. Ben Taieb and Koo [2019] relaxed the unbiasedness condition, and proposed `ERM` which optimizes the bias-variance trade-off by solving an empirical risk minimization problem. Rangapuram et al. [2021] proposed `HierE2E` which trains a single neural network on all time series together. It enforces coherence conditions in model training. Another end-to-end approach was proposed in Mancuso et al. [2021] where the reconciliation is imposed in a customized loss function of the neural network. A probabilistic top-down approach was proposed in Das et al. [2022] where a distribution of proportions is learnt by an RNN model to split the parent forecast among its children

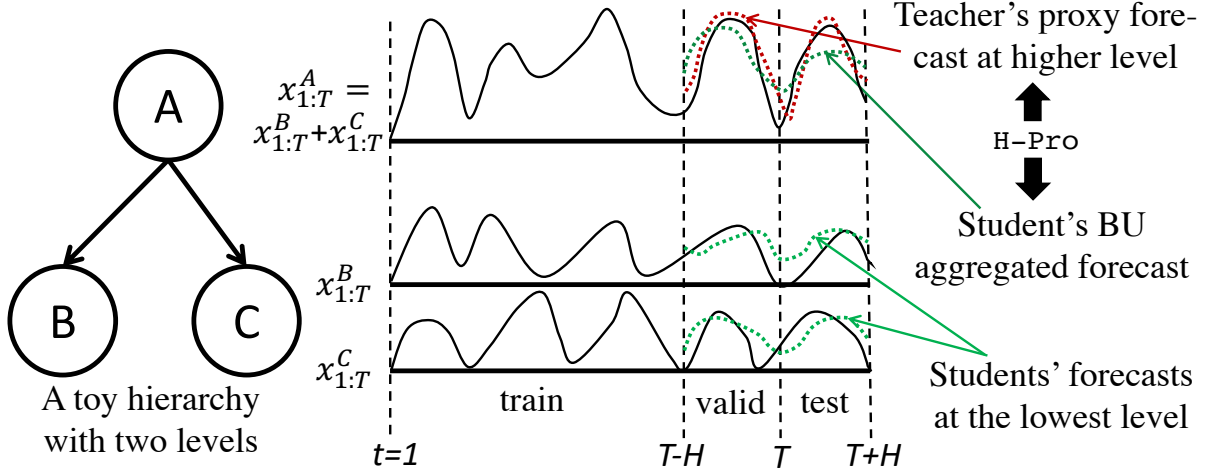


Figure 2: Visual explanation of H-PRO for a toy hierarchy. Temporal cross-validation performs HPO on the validation period with the actual ground truth data. H-PRO performs HPO on the test period with the teacher’s proxy forecast.

nodes. A top-down alignment-based reconciliation was developed in Anderer and Li [2021] where the lowest-level forecasts are adjusted based on the higher-level forecasts. The method employs a bias-controlling multiplier for the loss function of the lowest-level model, optimized by manual grid search.

4 H-Pro

We derive the HPO objective for conventional TCv, and then, extend it for H-PRO. For both cases, the models are trained at the lowest level, but their HPO techniques differ. Bottom-up (BU) aggregation is employed in both scenarios to generate coherent forecasts. We denote a learning algorithm by $\mathcal{A}(\mathcal{X}_{\text{train}}^L; \lambda)$, where $\mathcal{X}_{\text{train}}^L$ is the training data at the lowest level, λ denotes the hyperparameters, and we ignore the model’s parameters since those are learned in a separate optimization regime (not our focus). The goal of HPO is to find the best λ by minimizing an objective. For a given λ , \mathcal{A} provides the forecasting map f_λ as shown in (1). We subscript f with λ to concisely denote the forecasting model’s dependency on the algorithm’s hyperparameters.

4.1 HPO with temporal cross-validation (TCV)

Traditionally, TCv has been used to perform HPO and model selection for forecasting Salinas et al. [2020], Oreshkin et al. [2020]. Figure 2 shows the train, validation, and test splits for TCv with one validation window. Hence, those subsets can be expressed with time-ranges. For example, $\mathcal{X}_{\text{train}}^L = \{x_{1:T-H}^{L,j}\}_{j=1}^{N_L}$, and so on. We show the HPO objectives below for one validation window, but it can be generalized to multiple windows as well. Irrespective of the number of validation windows, the model is trained again on the entire train and validation period (i.e., on $\mathcal{X}_{\text{train+valid}}^L$) with the optimal hyperparameters λ^* to produce test forecasts, $\hat{x}_{T+1:T+H}^{L,j}$.

The HPO for TCv can target either the lowest-level error, or a hierarchically aggregated error (see Section 2.2). We denote the two variants as TCv-Lowest and TCv-Hier. Following Bergstra and Bengio [2012], the HPO objective for a single-validation TCv-Lowest can be written as

$$\begin{aligned} \lambda_{\text{TCV-Lowest}}^* &\approx \underset{\lambda \in \Lambda}{\operatorname{argmin}} \operatorname{mean}_{x^L \in \mathcal{X}_{\text{valid}}^L} [\mathcal{L}(x^L, \hat{x}^L)] \\ &= \underset{\lambda \in \Lambda}{\operatorname{argmin}} \frac{1}{N_L} \sum_{j=1}^{N_L} \mathcal{L}\left(x_{T-H+1:T}^{L,j}, f_\lambda\left(x_{1:T-H}^{L,j}\right)\right). \end{aligned} \quad (2)$$

While `TCV-Lowest` targets minimizing lowest-level error, `TCV-Hier` better targets the hierarchical forecasting objective as it aims to obtain low error at all levels. Formally,

$$\lambda_{\text{TCV-Hier}}^* \approx \underset{\lambda \in \Lambda}{\operatorname{argmin}} \frac{1}{L} \sum_{l=1}^L \left[\frac{1}{N_l} \times \sum_{j=1}^{N_l} \left[\mathcal{L} \left(x_{T-H+1:T}^{l,j}, \mathcal{B} \left(f_\lambda, \left\{ x_{1:T-H}^{L,i} \right\}_{i=1}^{N_L}, l, j \right) \right) \right] \right] \quad (3)$$

where, $\mathcal{B}(\cdot)$ is the bottom-up aggregation function which aggregates forecasts from the descendant leaf nodes to produce a forecast at node j of level l .

4.2 HPO with hierarchical proxy modeling

From (2) and (3) we can see that $\lambda_{\text{TCV-Hier}}^*$ and $\lambda_{\text{TCV-Lowest}}^*$ depend on the validation data $x_{T-H+1:T}^{l,j}$. Hence, a mismatch between the test series $x_{T+1:T+H}^{l,j}$ and validation series $x_{T-H+1:T}^{l,j}$ can lead to poor test performance. `H-PRO` attempts to address the issue based on the observation that, often, the higher-level aggregated time series are less irregular and have better predictability (e.g., in Makridakis et al. [2022]). It builds two sets of models: a *student model* as a base forecaster at the lowest level, and *teacher model(s)* as proxy forecasters at any (or all) higher levels (see Figure 2)². The student produces the final forecasts at all levels via bottom-up (BU) aggregation.

`H-PRO` proceeds as follows. The teacher model(s) are trained and their HPO is performed with `TCV`. Teacher’s forecasts are generated for the *test* period. We term these as teacher’s *proxy forecasts* since the student treats them as the actual ground truth for the *unknown* test period. The student is trained on the entire train and validation data at the lowest level, but its HPO is performed based on the proxy forecasts at higher levels. Intuitively, the student model is regularized in a way such that it tries to mimic the proxy forecasts of the teacher, but only at higher level(s) since teacher’s forecasts are *not* available at the lowest level. We hypothesize that even if we guide the student to produce accurate forecasts at higher level(s) for the test period, it would enable the student to produce accurate forecasts in all or at least some of the lower levels because the higher level forecasts are obtained by aggregating the lower level forecasts (Figure. 2).

Following (3), the `H-PRO` objective can be written as

$$\lambda_{\text{H-PRO}}^* \approx \underset{\lambda \in \Lambda}{\operatorname{argmin}} \sum_{l=1}^{L-1} \left[w(l) \cdot \frac{1}{N_l} \times \sum_{j=1}^{N_l} \left[\mathcal{L} \left(\tilde{x}_{T+1:T+H}^{l,j}, \mathcal{B} \left(f_\lambda, \left\{ x_{1:T}^{L,i} \right\}_{i=1}^{N_L}, l, j \right) \right) \right] \right] \quad (4)$$

where, $\tilde{x}_{T+1:T+H}^{l,j}$ denotes the teacher’s proxy forecasts at that node, and $w(l) \in [0, 1]$ assigns a confidence-weight on the teacher at level l . Hence, $\sum_{l=1}^{L-1} w(l) = 1$. It is evident that the optimal hyperparameters $\lambda_{\text{H-PRO}}^*$ depend on the teacher’s proxy forecasts $\tilde{x}_{T+1:T+H}^{l,j}$, and the bottom-up aggregated test forecast of the student. This removes the dependency of `H-PRO`-based HPO on the validation period.

Properties of `H-PRO`

We describe some characteristics of `H-PRO` which will help us understand its strength.

Definition 4.1 (Perfect teacher). *A perfect teacher generates proxy forecasts with zero error, i.e., $\forall l \in [L-1], j \in [N_l], \tilde{x}_{T+1:T+H}^{l,j} = x_{T+1:T+H}^{l,j}$.*

Definition 4.2 (OPT-BU). *The optimal bottom-up (BU)-aggregated student model is obtained by optimizing the hyperparameters of a student model, where the HPO objective minimizes a specified loss \mathcal{L} between the bottom-up*

²`H-PRO` is different from knowledge distillation Hinton et al. [2015]. `H-PRO` is developed for HPO and not for model training, it requires a hierarchical dataset, and it differs in the core algorithm.

Table 1: Datasets and models. $N_L = \#Series$ (lowest-level), $H =$ forecast horizon, $T + H =$ length of series, $L = \#Levels$.

Dataset	N_L	T	H	L	Teacher	Student
Tourism	56	28	8	4	DeepAR	DeepAR
Tour-L	304	216	12	8	Theta	(Theta+ LightGBM)
Wiki	150	365	1	5	DeepAR	DeepAR
Traffic	200	359	7	4	N-BEATS	LightGBM
M5	30490	1913	28	12	LightGBM	LightGBM

aggregated student forecasts and the ground truth data at the test period across all higher levels.

$$\lambda_{\text{OPT-BU}}^* \approx \underset{\lambda \in \Lambda}{\operatorname{argmin}} \frac{1}{L-1} \sum_{l=1}^{L-1} \left[\frac{1}{N_l} \times \sum_{j=1}^{N_l} \left[\mathcal{L} \left(x_{T+1:T+H}^{l,j}, \mathcal{B} \left(f_\lambda, \left\{ x_{1:T}^{L,i} \right\}_{i=1}^{N_L}, l, j \right) \right) \right] \right]. \quad (5)$$

Lemma 1. For a perfect teacher, if $w(l) = \frac{1}{L-1}, \forall l \in [L-1]$ in (4), the hyperparameters of the student model obtained by applying H-PRO are the same as that of the OPT-BU, i.e., $\lambda_{\text{H-PRO}}^* = \lambda_{\text{OPT-BU}}^*$.

The proof is in Appendix B. Lemma 1 implies that if the teacher is extremely accurate, H-PRO can regularize the student to have accurate aggregated forecasts at the higher levels. However, a perfect teacher is rare! The following theorem attempts to quantify the difference between the HPO objectives of H-PRO with an imperfect and a perfect teacher.

Theorem 1. Let $\epsilon_t^{l,j} = |x_t^{l,j} - \hat{x}_t^{l,j}|$ and $\delta_t^{l,j} = |x_t^{l,j} - \hat{x}_t^{l,j}|$ be point-wise absolute errors for the teacher and the BU-aggregated student forecasts at the j -th node of l -th level. Let \mathcal{E} denote the teacher’s aggregated mean squared error at all higher levels. Let \mathcal{O} and \mathcal{O}^* denote the HPO objectives of H-PRO and OPT-BU respectively. Let $w(l) = \frac{1}{L-1}, \forall l \in [L-1]$. Then, for mean squared error objective \mathcal{L} ,

$$|\mathcal{O} - \mathcal{O}^*| \leq \mathcal{E} + \frac{2}{L-1} \sum_{l=1}^{L-1} \frac{1}{N_l} \sum_{j=1}^{N_l} \frac{1}{H} \sum_{t=T+1}^{T+H} \epsilon_t^{l,j} \delta_t^{l,j} \quad (6)$$

The proof is in Appendix B. The second term in the RHS of (6) indicates an inter-related absolute error between the teacher and the BU-aggregated student forecasts. The significance of Theorem 1 is that if we can have reasonably accurate teacher ($\epsilon_t^{l,j} \rightarrow 0 \implies \mathcal{E} \rightarrow 0$), then, H-PRO’s objective is close to that of OPT-BU, leading to accurate forecasts at the higher levels. On the contrary, a suboptimal teacher can lead to inferior performance of the student. However, as explained above, the higher level time series generally possess better predictability, and we observe this phenomena in multiple datasets, which leads to superior performance of H-PRO in our extensive experiments (Section 5).

One notable point is that the student is *not* trained with proxy forecasts, but they are only regularized with them. The training is performed on the lowest-level’s ground truth data from the entire train and validation periods. Hence, H-PRO does not have any direct effect on the learned parameters of the student model, but only on its hyperparameters.

5 Experiments

5.1 Experimental setting

Datasets

We present extensive empirical evaluation on five publicly available datasets: Tourism Tourism Australia, Canberra [2005], Tourism-L Wickramasuriya et al. [2019], Wiki Wikistats [2016], Traffic Dua and Graff [2017], and M5 Makridakis et al. [2022]. The datasets are prepared according to Rangapuram et al. [2021]. A summary is given in Table 1, with more details in Appendix C. Tourism-L and Traffic are abbreviated as Tour-L and Traff, respectively for space constraints.

Forecasting models

Table 1 shows the models employed for different datasets. See Section 1 for references to the models. For the student, H-PRO works with any ML model that can be regularized by HPO. We validate the strength of H-PRO by employing two models as students: DeepAR and LightGBM. For Tourism-L data, the student is an ensemble of Theta Assimakopoulos and Nikolopoulos [2000] and LightGBM. For teacher, H-PRO works with both classical models that do not require HPO and complex ML models needing HPO. We employ Theta, DeepAR, LightGBM, and N-BEATS as teachers in different datasets. Note that an independent Theta model is built for each time series, while for all other models, a single model is trained on all time series collected from the suitable levels.

Teacher configuration

We explore two teacher configurations. (1) In H-PRO-Top, proxies from the top-most level is only utilized by the student, i.e., $w(1) = 1$, and $w(l) = 0, \forall 2 \leq l \leq L - 1$. (2) In H-PRO-Avg, proxy forecasts from more than one higher level are utilized by the student. Hence, $w(l) = 1/L_T, \forall 1 \leq l \leq L_T \leq L - 1$. We set $L_T = L - 1$ for Tourism, Wiki, and Traffic data, and $L_T = 5$ for Tourism-L and M5 data. The reason for choosing lower L_T for Tourism-L and M5 is that they have relatively deep hierarchies, and training a teacher with data from levels very deep in the tree conflicts with our hypothesis of training the teacher with less sparse data.

Performance metric

We adopt the scale-agnostic Root Mean Squared Scaled Error (RMSSE) as our base metric (used in M5 competition). For a single time series $x^{l,j}$, it is defined as: $r^{l,j} = \sqrt{e/e_{\text{naive}}}$, where $e = \frac{1}{H} \sum_{t=T+1}^{T+H} (x_t^{l,j} - \hat{x}_t^{l,j})^2$, and $e_{\text{naive}} = \frac{1}{T-1} \sum_{t=2}^T (x_t^{l,j} - x_{t-1}^{l,j})^2$. For multiple series, generally a weighted average is considered. RMSSE at a certain level l is given by, $r^l = \sum_j \alpha_j \times r^{l,j}$. In our experiments, $\alpha_j = 1/N_l$ for all datasets except for M5. A special weighting scheme is used in M5 as described in Makridakis et al. [2022]. As introduced in Section 2, we adopt mean aggregation across levels, and employ **Hierarchical RMSSE**, $R_H = \frac{1}{L} \sum_{l=1}^L r^l$ as our primary metric. A lower value of R_H is preferred. Note that H-PRO and other methods implemented here always produce coherent forecasts across hierarchies via reconciliation.

5.2 HPO framework

We adopt Random search Bergstra and Bengio [2012] and Hyperopt Bergstra et al. [2013] as search algorithms, and use RayTune Liaw et al. [2018] to perform end-to-end training and HPO in a distributed Kubernetes cluster. More details about HPO trials and grids for every model are given in Appendix C. We employ two model selection frameworks: (a) The *Standard* approach selects the best HPO trial based on the aggregated TCV/H-PRO objective across the entire forecast horizon. (b) The *Per-offset (PO)* method selects the best trial for each offset time-point in the horizon based on TCV/H-PRO objective at that time, and then concatenates the individual predictions to generate the forecast for the entire horizon. The second method does more granular selection from a pool of HPO trials.

5.3 Detailed results on benchmark datasets

Table 2 shows *test* Hierarchical RMSSE for H-PRO, state-of-the-art, and baseline methods. We show mean and standard deviation (“std”) of the metric over multiple (3/4) HPO runs with different seeds (some classical forecasters have std=0 because of deterministic behavior). A single HPO run generally contains hundreds of trials (see Appendix C).

Gold

In Table 2, the row with tag “Gold” shows the result of base (student) forecasters with HPO performed on the *test* set. It gives lower bounds on the error achievable by the students. Hence, our methods (with tags “Baselines” and “Ours”) should not be able to outperform the Gold R_H scores.

State-of-the-arts (SOTAs)

Following Rangapuram et al. [2021], we adopt three reconciliation methods for comparison: naive bottom-up (BU), MinT, and ERM (see Section 3). We present results on multiple combinations of base forecasters and reconciliation methods. We choose two classical forecasters: ARIMA and exponential smoothing (a.k.a. ETS), and present results in combination with BU, MinT, and ERM. We experimented with two variants of MinT: MinT-shr and MinT-ols, and report the best one in the paper. We also present the performance of PERMBU Taieb et al. [2017] in combination

Table 2: Test Hierarchical RMSSE (R_H) (mean \pm std) for different forecasters with their reconciliation methods in four datasets. The best score is in **bold**, best baseline is in *italics*, and best SOTA is underlined. PERMBU failed in Tourism-L data.

Tag	Forecaster	Recon- ciliation	Tourism	Tourism-L	Wiki	Traffic
Gold	HPO on test	BU	0.4668 \pm 0.0117	0.4907 \pm 0.0018	0.3199 \pm 0.0076	0.3736 \pm 0.0103
State-of-the-arts (SOTAs)	ARIMA	BU	0.5434 \pm 0.0000	0.5462 \pm 0.0000	0.7533 \pm 0.0000	0.5353 \pm 0.0000
	ETS	BU	0.5264 \pm 0.0000	0.5204 \pm 0.0000	0.7180 \pm 0.0000	0.4954 \pm 0.0000
	ARIMA	MinT	0.5481 \pm 0.0000	<u>0.4960\pm0.0000</u>	0.4282 \pm 0.0000	0.4556 \pm 0.0000
	ETS	MinT	0.5021 \pm 0.0000	0.5007 \pm 0.0000	0.4455 \pm 0.0000	0.4683 \pm 0.0000
	ARIMA	ERM	2.8064 \pm 0.0000	1.8756 \pm 0.0000	<u>0.3940\pm0.0000</u>	0.9248 \pm 0.0000
	ETS	ERM	10.2069 \pm 0.0000	1.9253 \pm 0.0000	0.4229 \pm 0.0000	1.4080 \pm 0.0000
	PERMBU	MinT	<u>0.5011\pm0.0140</u>	–	0.4244 \pm 0.0436	0.4704 \pm 0.0132
	DeepAR	N/A	0.6236 \pm 0.0419	0.5749 \pm 0.0140	0.4896 \pm 0.0678	0.4352 \pm 0.0229
	DeepVAR+	Inherent	0.6757 \pm 0.0602	0.6264 \pm 0.0349	0.7527 \pm 0.1476	0.4693 \pm 0.0629
	HierE2E	Inherent	0.5713 \pm 0.0411	0.6201 \pm 0.0257	0.5054 \pm 0.0905	<u>0.3910\pm0.0217</u>
Baselines	TCV-Lowest	BU	0.8996 \pm 0.2112	0.5101 \pm 0.0009	<i>0.3904\pm0.0609</i>	<i>0.4014\pm0.0073</i>
	TCV-Lowest-PO	BU	0.8313 \pm 0.1558	0.5128 \pm 0.0011	<i>0.3904\pm0.0609</i>	0.4077 \pm 0.0146
	TCV-Hier	BU	0.6966 \pm 0.1519	<i>0.4915\pm0.0020</i>	0.4439 \pm 0.0504	0.4128 \pm 0.0386
	TCV-Hier-PO	BU	<i>0.6770\pm0.1789</i>	0.4997 \pm 0.0013	0.4439 \pm 0.0504	0.4920 \pm 0.0398
Ours	H-Pro-Avg	BU	0.5310 \pm 0.0223	0.4907\pm0.0018	0.3242 \pm 0.0085	0.3827 \pm 0.0093
	H-Pro-Avg-PO	BU	0.4673\pm0.0094	0.4935 \pm 0.0005	0.3242 \pm 0.0085	0.3766\pm0.0034
	H-Pro-Top	BU	0.5138 \pm 0.0179	0.4953 \pm 0.0055	0.3230\pm0.0072	0.3869 \pm 0.0070
	H-Pro-Top-PO	BU	0.5158 \pm 0.0178	0.4924 \pm 0.0007	0.3230\pm0.0072	0.3812 \pm 0.0193

 Table 3: Level-wise mean RMSSE for the best H-Pro, best baseline, and best SOTA methods. The best score is **bolded**, second best is underlined. Full table with standard deviation is in Appendix C. “–” denotes unavailability of levels in a dataset.

Data	Forecaster	L1	L2	L3	L4	L5	L6	L7	L8
Tour	Ours (H-Pro-Avg-PO)	0.3383	0.4251	0.5336	0.5723	–	–	–	–
	Best baseline (TCV-Hier-PO)	0.6473	0.7137	0.6836	0.6635	–	–	–	–
	Best SOTA (PERMBU-MinT)	<u>0.3843</u>	<u>0.4766</u>	<u>0.5539</u>	<u>0.5895</u>	–	–	–	–
Tour-L	Ours (H-Pro-Avg)	<u>0.1812</u>	0.3861	<u>0.4737</u>	0.5749	0.4409	0.5575	0.6405	0.6704
	Best baseline (TCV-Hier)	0.1838	<u>0.3869</u>	0.4732	<u>0.5759</u>	<u>0.4433</u>	<u>0.5579</u>	<u>0.6403</u>	<u>0.6705</u>
	Best SOTA (ARIMA-MinT)	0.1486	0.4079	0.4986	0.5812	0.4482	0.5757	0.6345	0.6732
Wiki	Ours (H-Pro-Top)	0.1954	0.3007	<u>0.3256</u>	0.442	<u>0.3515</u>	–	–	–
	Best baseline (TCV-Lowest-PO)	0.3947	0.4027	0.3502	<u>0.4558</u>	0.3485	–	–	–
	Best SOTA (ARIMA-ERM)	0.1615	<u>0.3132</u>	0.3165	0.5827	0.5960	–	–	–
Traff	Ours (H-Pro-Avg-PO)	0.1764	0.2103	<u>0.2865</u>	0.8332	–	–	–	–
	Best baseline (TCV-Lowest)	<u>0.2324</u>	0.2627	0.3233	0.7870	–	–	–	–
	Best SOTA (HierE2E)	0.2329	<u>0.2423</u>	0.2726	<u>0.8163</u>	–	–	–	–

with MinT. For DNN-based methods, we compare with DeepAR without any reconciliation Salinas et al. [2019], DeepVAR+ with reconciliation as a post-processing Rangapuram et al. [2021], and the recent HierE2E method Rangapuram et al. [2021]. For probabilistic forecasters (like HierE2E), we take the mean forecast as point forecast.

Baselines

Our baselines are direct application of student models along with BU reconciliation. TCV-Lowest and TCV-Hier refer to TCV-based models targeting the lowest-level’s RMSSE and hierarchical RMSSE respectively (see Section 4.1). TCV-Lowest-PO and TCV-Hier-PO refer to their extensions with per-offset model section (see Section 5.2). We employ single and multiple (up to 4) validation windows for the baselines, and report the best results.

Table 4: Hierarchical RMSSE, R_H (M5 official metric) and level-wise weighted RMSSE for H-PRO, SOTA, and baseline (“Base.”) in M5 dataset for “department+store” ensemble student model. The best score is in **bold**. Full table is in Appendix C.

Tag	Method	R_H	L1	L2	L3	L4	L5	L6	L7	L8	L9	L10	L11	L12
Gold	HPO on test	0.512	0.186	0.294	0.387	0.237	0.328	0.370	0.455	0.465	0.561	1.001	0.954	0.903
SOTA	M5 winner	<u>0.520</u>	0.199	0.310	0.400	0.277	0.366	0.390	0.474	0.480	0.573	0.966	0.929	0.884
Base.	TCV-Hier	0.534	0.230	0.327	0.410	0.280	0.363	0.403	0.483	0.489	0.580	0.999	0.951	0.899
Ours	H-Pro-Top	0.512	0.186	0.294	0.386	0.237	0.329	0.370	0.456	0.464	0.561	1.003	0.955	0.903
	H-Pro-Avg	0.534	0.231	0.327	0.409	0.280	0.363	0.402	0.483	0.488	0.580	1.000	0.951	0.899
	H-Pro-Top-PO	0.521	0.189	0.305	0.398	0.247	0.339	0.383	0.468	0.477	0.572	1.009	0.961	0.909
	H-Pro-Avg-PO	0.534	0.227	0.325	0.408	0.277	0.362	0.401	0.483	0.486	0.580	1.001	0.953	0.901

Observation on Hierarchical RMSSE

We build four versions of H-PRO as shown in Table 2 with “Ours” tag: H-PRO-Avg and H-PRO-Top as explained in Section 5.1, and their per-offset extensions H-PRO-Avg-PO and H-PRO-Top-PO. We can see that H-PRO outperforms all the baselines and the SOTAs in all four datasets. H-PRO achieves this performance with off-the-shelf forecasting models, which highlights its strength as an HPO technique. Moreover, all four datasets have different characteristics, e.g., Traffic and Tourism have strong seasonality while Wiki does not. Despite that H-PRO is able provide superior performance. This empirically validates our initial hypothesis that the better predictability at the higher levels can help learn accurate forecasters (teachers) at those levels, which can in turn help regularize lowest-level base (student) forecasters. Note that we do not use the teacher after H-PRO is completed, and the student itself can produce accurate and coherent forecasts across all levels. Another observation is that the per-offset (PO) model selection can be helpful sometimes for H-PRO as well as the baseline TCV methods. Note that for Wiki, the per-offset extension achieves the same result as the normal version because the horizon, $H = 1$. Comparing H-PRO-Top and H-PRO-Avg, we see that their relative performances vary across datasets. Hence, a detailed study will be presented in Section 5.5.

Observation on level-wise RMSSE

Table 3 shows the mean RMSSE for the best variant of H-PRO, the best baseline, and the best SOTA method in the above four datasets. For Tourism and Tourism-L data, H-PRO outperforms the contenders in most of the levels. For Wiki and Traffic data, occasionally the best score is achieved by one of the best competing methods. Out of total 21 levels, our method achieves the best performance in 13 levels, and the second best in 6 out of remaining 8 levels.

5.4 Result on large-scale retail forecasting

Here we validate our method in a large-scale retail forecasting dataset ($\sim 43K$ time series, 5.4 years of daily data) from the M5 accuracy competition. The winning methods in M5 demonstrated superior performance by the models built after clustering the data based on certain aggregated level ids. Hence, we perform “department”-wise and “store”-wise clustering, and train one independent H-PRO model for each cluster. We then ensemble these two forecasts to obtain our final result. We present the Hierarchical and level-wise RMSSE for the “department+store” ensemble model in Table 4. We can see that H-PRO-Top outperforms the M5 winning method Makridakis et al. [2022] by approximately 2% in the Hierarchical RMSSE (R_H), the primary metric used in the competition. It is also close to the Gold number. H-PRO-Top shows superior performance in level-wise RMSSE outperforming the winning method in the top 9 levels. A slight degradation in performance is observed at lower levels, possibly because the effect of the proxy is not being transmitted from the top-most to the lowest level due to the complicated and deep M5 hierarchy. Although, we should note that, in the M5 competition, the methods that achieved superior performance in the lower levels could not get the same in higher levels, and that was also reflected in their degraded Hierarchical RMSSE scores.

5.5 Discussion and ablation studies

Teacher performance

In the above experiments, we select the teacher models through temporal cross-validation with one or (if length permits) multiple validation windows. Table 5 shows the level-wise test RMSSE of the selected teachers in different datasets. In Tourism, Traffic, and Wiki, since the level-wise RMSSE of the teacher is better than the TCV baseline

Table 5: Teacher’s test RMSSE at different higher levels. Levels denoted with “–” were not used by the teacher.

Data	L1	L2	L3	L4	L5
Tour	0.3395	0.4297	0.5239	–	–
Tour-L	0.2044	0.4572	0.5458	0.6260	0.5180
Wiki	0.0825	0.3291	0.2710	0.4396	–
Traff	0.1029	0.1443	0.2299	–	–
M5	0.1832	0.6419	0.5850	0.4958	0.5871

Table 6: Hierarchical RMSSE of ensemble models (1) to (4).

Data	(1)	(2)	(3)	(4)	SOTA	Baseline
Tour	0.506	0.479	0.483	0.486	0.501	0.677
Tour-L	0.491	0.488	0.488	0.488	0.496	0.491
Wiki	0.323	0.323	0.323	0.352	0.394	0.390
Traff	0.378	0.373	0.366	0.370	0.391	0.401
M5	0.520	0.520	0.519	0.521	0.520	0.534

(from Table 3), H-PRO gets relatively large improvement ($\sim 7\%$, 4% , 18%) from SOTAs. On the other-hand, for Tourism-L and M5, where the teacher’s level-wise performance is not superior to the TCv baseline, we observe only marginal improvement ($\sim 1\%$ and 2%) from SOTAs. An important observation from Table 5 and 3 is that a student can perform better than its teacher in some of the higher levels, even though it is regularized with the teacher’s proxy forecasts. This can be attributed to the student’s learning ability from the lowest-level data while regularized by the aggregated signals from the teacher.

Teacher selection and ensemble modeling

As shown in Theorem 1, an accurate teacher helps the student to produce accurate higher-level forecasts. However, in Section 5.3 and 5.4, we saw that the two variants of H-PRO (H-PRO-Avg and H-PRO-Top) built with two configurations of the teacher can achieve the best results interchangeably across datasets. For example, in M5, teacher’s test accuracy in L1 is good but poor in other levels. Hence, we observe H-PRO-Top outperforms SOTA while H-PRO-Avg fails, as shown in Table 4. In practice, since the teacher’s test accuracy is not known, we would need a mechanism to achieve stable performance of H-PRO Top and H-PRO-Avg across datasets. To address this, we build ensemble models between different variants of H-PRO. We use the mean of the forecasts from multiple models for ensembles. As an ablation study, we also build ensemble models between H-PRO and TCv baselines. We denote these ensembles with the following names for concise representation in Table 6. (1) H-PRO-Avg and H-PRO-Top, (2) H-PRO-Avg-PO and H-PRO-Top-PO, (3) 1 and 2, (4) 3 and the best TCv baseline as obtained in Table 2. In all datasets, the ensembles perform better than the baselines. We can see that the ensemble among all H-PRO variants (id=3) outperforms the best SOTAs and baselines across all five datasets, and hence, can be considered a more stable version of H-PRO, which is more robust to possible sub-optimal teacher performance. Moreover, ensembles of H-PRO variants and TCv improve the performance of the latter, which is beneficial as it shows complementary information was integrated by our approach.

Adaptation to new test window

Although, H-PRO is targeted to a particular test-window, we can easily tune it to new test windows by leveraging the saved models from the previous HPO run. H-PRO only requires recomputing the predictions and evaluating the HPO objective for every trial in the past HPO run to select the best model for the new test window. Thus, retraining for all the HPO trials is not mandatory for H-PRO, leading to faster adaptation to newer test windows. We should note that, often in forecasting, the immediate past is utilized in training. In that scenario, H-PRO and TCv both need to rerun full HPO.

6 Concluding remarks

We proposed a hierarchical proxy-guided HPO method for hierarchical time series forecasting to mitigate the perennial problem of data mismatch between validation and test periods in real-life time series. We provided theoretical justification of the approach along with extensive empirical evidence. The proposed method outperforms well-established SOTAs in five different datasets. A future extension can be on formulating a fractional confidence score for the teacher

at a certain higher-level node so that suboptimal teacher forecasts can be given lower priority during the HPO of the student model.

References

- Spyros Makridakis, Evangelos Spiliotis, and Vassilios Assimakopoulos. M5 accuracy competition: Results, findings, and conclusions. *International Journal of Forecasting*, 2022. ISSN 0169-2070. URL <https://www.sciencedirect.com/science/article/pii/S0169207021001874>. <https://doi.org/10.1016/j.ijforecast.2021.11.013>.
- R.J. Hyndman and G. Athanasopoulos, editors. *Forecasting: principles and practice*. OTexts: Melbourne, Australia, 2021. OTexts.com/fpp3.
- David Salinas, Valentin Flunkert, Jan Gasthaus, and Tim Januschowski. Deepar: Probabilistic forecasting with autoregressive recurrent networks. *International Journal of Forecasting*, 36(3):1181–1191, 2020.
- Boris N Oreshkin, Dmitri Carпов, Nicolas Chapados, and Yoshua Bengio. N-beats: Neural basis expansion analysis for interpretable time series forecasting. In *International Conference on Learning Representations*, 2020. <https://openreview.net/forum?id=r1ecqn4YwB>.
- Haoyi Zhou, Shanghang Zhang, Jieqi Peng, Shuai Zhang, Jianxin Li, Hui Xiong, and Wancai Zhang. Informer: Beyond efficient transformer for long sequence time-series forecasting. In *Proceedings of the AAAI Conference on Artificial Intelligence*, volume 35, pages 11106–11115, 2021.
- Syama Sundar Rangapuram, Lucien D Werner, Konstantinos Benidis, Pedro Mercado, Jan Gasthaus, and Tim Januschowski. End-to-end learning of coherent probabilistic forecasts for hierarchical time series. In *International Conference on Machine Learning*, pages 8832–8843. PMLR, 2021.
- Biswajit Paria, Rajat Sen, Amr Ahmed, and Abhimanyu Das. Hierarchically regularized deep forecasting. *arXiv preprint arXiv:2106.07630*, 2021.
- Abhimanyu Das, Weihao Kong, Biswajit Paria, and Rajat Sen. A top-down approach to hierarchically coherent probabilistic forecasting. *arXiv preprint arXiv:2204.10414*, 2022.
- Paolo Mancuso, Veronica Piccialli, and Antonio M Sudoso. A machine learning approach for forecasting hierarchical time series. *Expert Systems with Applications*, 182:115102, 2021. <https://doi.org/10.1016/j.eswa.2021.115102>.
- Vedat Akgiray. Conditional heteroscedasticity in time series of stock returns: Evidence and forecasts. *Journal of business*, 62(1):55–80, 1989.
- Shanika L Wickramasuriya, George Athanasopoulos, and Rob J Hyndman. Optimal forecast reconciliation for hierarchical and grouped time series through trace minimization. *Journal of the American Statistical Association*, 114(526):804–819, 2019.
- Souhaib Ben Taieb and Bonsoo Koo. Regularized regression for hierarchical forecasting without unbiasedness conditions. In *Proceedings of the 25th ACM SIGKDD International Conference on Knowledge Discovery & Data Mining*, pages 1337–1347, 2019.
- Matthias Anderer and Feng Li. Forecasting reconciliation with a top-down alignment of independent level forecasts. *arXiv preprint arXiv:2103.08250*, 2021.
- James Bergstra and Yoshua Bengio. Random search for hyper-parameter optimization. *Journal of machine learning research*, 13(2):281–305, 2012.
- Geoffrey Hinton, Oriol Vinyals, Jeff Dean, et al. Distilling the knowledge in a neural network. *arXiv preprint arXiv:1503.02531*, 2(7), 2015.
- Tourism Australia, Canberra. Tourism research australia (2005), travel by australians. Accessed at <https://robjhyndman.com/publications/hierarchical-tourism/>, 2005.
- Wikistats. Wikistats: Pageview complete dumps, Wikimedia Analytics team. Accessed at https://dumps.wikimedia.org/other/pageview_complete/readme.html, 2016.
- Dheeru Dua and Casey Graff. UCI machine learning repository. <http://archive.ics.uci.edu/ml>, 2017. University of California, Irvine, School of Information and Computer Sciences".
- Vassilis Assimakopoulos and Konstantinos Nikolopoulos. The theta model: a decomposition approach to forecasting. *International journal of forecasting*, 16(4):521–530, 2000.
- James Bergstra, Daniel Yamins, and David Cox. Making a science of model search: Hyperparameter optimization in hundreds of dimensions for vision architectures. In *Proceedings of the 30th International Conference on Machine Learning*, volume 28, pages 115–123. PMLR, 2013.

Richard Liaw, Eric Liang, Robert Nishihara, Philipp Moritz, Joseph E Gonzalez, and Ion Stoica. Tune: A research platform for distributed model selection and training. *arXiv preprint arXiv:1807.05118*, 2018.

Souhaib Ben Taieb, James W Taylor, and Rob J Hyndman. Coherent probabilistic forecasts for hierarchical time series. In *International conference on machine learning*, pages 3348–3357. PMLR, 2017.

David Salinas, Michael Bohlke-Schneider, Laurent Callot, Roberto Medico, and Jan Gasthaus. High-dimensional multivariate forecasting with low-rank gaussian copula processes. *Advances in neural information processing systems*, 32, 2019.

Appendix

A Advantages of H-Pro over existing reconciliation methods

State-of-the-art reconciliation methods like `MinT` and `ERM` try to factor in forecasts at all levels to derive the final adjusted forecasts, but these have several shortcomings. First, they are generally not scalable to large number of time series, since they at least require fitting parameter matrices that have size on the order of $N \times N$ where N is the number of base time series. This fitting essentially requires multiple matrix inversions of matrices of this size (which has complexity more than $O(N^4)$), or for the best performing `ERM`, solving an even bigger regression problem with $O(TN^2)$ data points (where T is the number of historical time points) and $O(N^2)$ variables. Additionally they add significant complexity to the forecast process (i.e., getting all hierarchy forecasts on historical data, fitting the reconciliation model, getting forecasts and applying reconciliation model at test time to adjust base forecasts, *etc.*), and can suffer from overfitting especially with modern ML and DL forecasting approaches that may have close to zero training error, since typically training data forecasts are used to fit the reconciliation model.

Furthermore, both these and the simpler top-down / middle-out reconciliation approaches use fixed linear combinations of different series' forecasts (a single series in the case of top-down and middle-out) to get the adjusted base forecasts, which can be insufficient to accurately predict the base level when the relationship between the levels is more complex (e.g., nonlinear) or changes over time, which is a common case as different local effects can cause proportions relative to aggregates to shift (e.g., consider events like promotion, price change, or advertisement in a retail setting, causing demand and sales for one product to shift to another).

`H-Pro` on the other hand adjusts the selected base level forecasters directly by leveraging aggregate-level information, hence, can still have time-evolving changes in relative proportions for base level series that factor in all local information. Additionally it avoids having to fit a reconciliation model and apply a complex reconciliation process so it is much more scalable, simpler, and easier to use. While it does require some aggregate level forecasts, these are only needed for the test periods used for model selection.

B Proofs

B.1 Proof of Lemma 1

This can be proved trivially, by employing Definition 4.1 in (4), and comparing with (5).

B.2 Proof of Theorem 1

Proof. Following (4),

$$\mathcal{O} = \frac{1}{L-1} \sum_{l=1}^{L-1} \frac{1}{N_l} \sum_{j=1}^{N_l} \frac{1}{H} \sum_{t=T+1}^{T+H} \left(\tilde{x}_t^{l,j} - \hat{x}_t^{l,j} \right)^2, \quad (7)$$

where, we denote $\hat{x}_t^{l,j} = \mathcal{B} \left(f_\lambda, \left\{ x_{1:T}^{L,i} \right\}_{i=1}^{N_L}, l, j \right)$ for compactness. Following (5),

$$\mathcal{O}^* = \frac{1}{L-1} \sum_{l=1}^{L-1} \frac{1}{N_l} \sum_{j=1}^{N_l} \frac{1}{H} \sum_{t=T+1}^{T+H} \left(x_t^{l,j} - \hat{x}_t^{l,j} \right)^2. \quad (8)$$

To make the equations concise, let

$$\mathcal{S}(\cdot) = \frac{1}{L-1} \sum_{l=1}^{L-1} \frac{1}{N_l} \sum_{j=1}^{N_l} \frac{1}{H} \sum_{t=T+1}^{T+H} (\cdot). \quad (9)$$

Hence,

$$\mathcal{O} = \mathcal{S} \left(\tilde{x}_t^{l,j} - \hat{x}_t^{l,j} \right)^2 \quad (10)$$

$$\mathcal{O}^* = \mathcal{S} \left(x_t^{l,j} - \hat{x}_t^{l,j} \right)^2. \quad (11)$$

Hence,

$$\begin{aligned}
 & \left| \mathcal{O} - \mathcal{O}^* \right| \\
 &= \left| \mathcal{S} \left(\left(\tilde{x}_t^{l,j} - \hat{x}_t^{l,j} \right)^2 - \left(x_t^{l,j} - \hat{x}_t^{l,j} \right)^2 \right) \right| \\
 &= \left| \mathcal{S} \left(\left(\tilde{x}_t^{l,j} - x_t^{l,j} \right) \left(\tilde{x}_t^{l,j} - 2\hat{x}_t^{l,j} + x_t^{l,j} \right) \right) \right| \\
 &= \left| \mathcal{S} \left(\left(\tilde{x}_t^{l,j} - x_t^{l,j} \right) \left(2 \left(x_t^{l,j} - \hat{x}_t^{l,j} \right) + \left(\tilde{x}_t^{l,j} - x_t^{l,j} \right) \right) \right) \right|.
 \end{aligned}$$

Applying triangle inequality ($|a + b| \leq |a| + |b|$),

$$\begin{aligned}
 & \left| \mathcal{O} - \mathcal{O}^* \right| \\
 &\leq \mathcal{S} \left(\left| \left(\tilde{x}_t^{l,j} - x_t^{l,j} \right) \left(2 \left(x_t^{l,j} - \hat{x}_t^{l,j} \right) + \left(\tilde{x}_t^{l,j} - x_t^{l,j} \right) \right) \right| \right) \\
 &= \mathcal{S} \left(\left| \tilde{x}_t^{l,j} - x_t^{l,j} \right| \left| 2 \left(x_t^{l,j} - \hat{x}_t^{l,j} \right) + \left(\tilde{x}_t^{l,j} - x_t^{l,j} \right) \right| \right).
 \end{aligned}$$

Applying triangle inequality again on the inner term,

$$\begin{aligned}
 & \left| \mathcal{O} - \mathcal{O}^* \right| \\
 &\leq \mathcal{S} \left(\left| \tilde{x}_t^{l,j} - x_t^{l,j} \right| \left(\left| 2 \left(x_t^{l,j} - \hat{x}_t^{l,j} \right) \right| + \left| \tilde{x}_t^{l,j} - x_t^{l,j} \right| \right) \right) \\
 &= \mathcal{S} \left(\left| \tilde{x}_t^{l,j} - x_t^{l,j} \right|^2 \right) + 2\mathcal{S} \left(\left| \tilde{x}_t^{l,j} - x_t^{l,j} \right| \left| x_t^{l,j} - \hat{x}_t^{l,j} \right| \right)
 \end{aligned}$$

(12)

Let \mathcal{E} denote the aggregated mean squared error of teacher’s proxy forecasts in all higher levels. Formally,

$$\mathcal{E} = \frac{1}{L-1} \sum_{l=1}^{L-1} \frac{1}{N_l} \sum_{j=1}^{N_l} \frac{1}{H} \sum_{t=T+1}^{T+H} \left(\tilde{x}_t^{l,j} - x_t^{l,j} \right)^2 \quad (13)$$

$$= \mathcal{S} \left(\left| \tilde{x}_t^{l,j} - x_t^{l,j} \right|^2 \right). \quad (14)$$

Substituting (14) in (12),

$$\begin{aligned}
 & \left| \mathcal{O} - \mathcal{O}^* \right| \\
 &\leq \mathcal{E} + \frac{2}{L-1} \sum_{l=1}^{L-1} \frac{1}{N_l} \sum_{j=1}^{N_l} \frac{1}{H} \sum_{t=T+1}^{T+H} \epsilon_t^{l,j} \delta_t^{l,j}.
 \end{aligned}$$

□

C Detailed experiments and results

C.1 Dataset details

We present the details of all datasets in the Table 7. Note that, in the column “Hierarchy description”, “__all_ids__” represent the top-most level, and “id” represents the lowest level.

C.2 HPO details

DeepAR

We use randomized search Bergstra and Bengio [2012] with 500 trials per HPO run. We run the entire HPO three times with three different random seeds. We implement DeepAR with the GluonTS toolkit (<https://ts.gluon.ai/stable/index.html>). Table 8 depicts the HPO grid used for the DeepAR model. The same search is employed for both student and teacher. The names of the hyperparameter are according GluonTS version 0.9.4.

N-BEATS

We use randomized search Bergstra and Bengio [2012] with 32 trials per HPO run. The reason for low number of trials per HPO run is the expensive computational demand because, running a single N-BEATS trial involves training hundreds of models due to ensemble modeling. We run the entire HPO three times with three different random seeds. We implement N-BEATS with the GluonTS toolkit (<https://ts.gluon.ai/stable/index.html>). Table 9 depicts the HPO grid used for the N-BEATS model. The names of the hyperparameter are according GluonTS version 0.9.4.

LightGBM

For LightGBM, we adopt different HPO configuration for different methods based on the computational demand. For LightGBM’s Traffic and Tourism student model, we use Hyperopt Bergstra et al. [2013] search with 100 trials on the hpo grid mentioned in Table. 10. Since the computational demand for M5 student model was very expensive, we selected a small grid with 32 combinations as mentioned in Table. 12 and we exercised a full grid search on this space. For LightGBM’s M5 teacher model, we use Hyperopt with 100 trials on the hpo grid mentioned in Table. 11.

We implement LightGBM using Ray distributed LightGBM (<https://docs.ray.io/en/latest/ray-more-libs/lightgbm-ray.html>). We enable multi-step forecast via. single-shot LightGBM regressor approach where we consider lag features (shifted back by forecast horizon), attributes (if available, e.g., in M5 data), and exogenous features (if available, e.g., in M5 data) as input features to predict a point forecast for every time-point in the forecast horizon.

C.3 Detailed result for level-wise performances on benchmark datasets

Please refer to Table 13 for the detailed level-wise test RMSSE on Tourism, Tourism-L, Wiki, and Traffic datasets.

C.4 Detailed result on M5 dataset

Please refer to Table 14 for the detailed cluster-wise M5 results. Experiments are conducted with 4 random seeds to derive the mean and standard deviation.

C.5 Detailed result on ensemble modeling

Table 15 shows the mean±standard deviation of Hierarchical RMSSE, R_H of ensemble models with ids: (1) H-Pro-Avg and H-Pro-Top, (2) H-Pro-Avg-PO and H-Pro-Top-PO, (3) 1 and 2, (4) 3 and the best TCV baseline as obtained in Table 2.

Table 7: Details of all datasets used in the experiment.

Dataset	Train length, T	Horizon, H	Frequency	Intermittency at lowest level?	Num. of hierarchy levels, L	Num. of lowest-level series, N_L	Num. of aggregated series	Total num. of series	Num. of validation windows for TCV	Hierarchy description	Other information
Tourism	28	8	Quarterly	No	4	56	33	89	1	L1: ["-all-ids-"] L2: ["purpose"] L3: ["state", "purpose"] L4: ["id"] = ["state", "purpose", "city vs noncity"]	Australian tourism flows from 1998 to 2006.
Tourism-L	216	12	Monthly	No	8	304	251	555	3	L1: ["-all-ids-"] L2: ["state"] L3: ["zone"] L4: ["region"] L5: ["purpose"] L6: ["state", "purpose"] L7: ["zone", "purpose"] L8: ["id"] = ["region", "purpose"]	Australian tourism flows from 1998 to 2016. Purpose-wise aggregation levels: 4 purposes. Location-wise aggregation levels: 7 states, 27 zones, 76 regions. Student cluster ids = (state, purpose)
Wiki	365	1	Daily	No	5	150	49	199	3	L1: ["-all-ids-"] L2: ["country-code"] L3: ["country-code", "access"] L4: ["country-code", "access", "agent"] L5: ["id"]	Daily views for 145K Wikipedia articles from July, 2015 to December, 2016. We follow Ben Taieb and Koo [2019] to create a subset of data containing 150 lowest-level series.
Traffic	359	7	Daily	No	4	200	7	207	3	L1: ["-all-ids-"] L2: ["second-level-id"] L3: ["third-level-id"] L4: ["id"]	Occupancy rate of car lanes on Bay Area freeways. Following Ben Taieb and Koo [2019], we create a subset of data. Student cluster ids= (second-level-id, third-level-id)
M5	1913	28	Daily	Yes	12	30490	39791	42840	3	L1: ["-all-ids-"] L2: ["state-id"] L3: ["store-id"] L4: ["cat-id"] L5: ["dept-id"] L6: ["state-id", "cat-id"] L7: ["state-id", "dept-id"] L8: ["store-id", "cat-id"] L9: ["store-id", "dept-id"] L10: ["item-id"] L11: ["item-id", "state-id"] L12: ["id"] = ["item-id", "store-id"]	Unit sales of products sold in Walmart, USA, organized in the form of grouped time series. Category-wise aggregation levels: 3 categories, 7 departments. Location-wise aggregation levels: 10 stores, 3 States. Student cluster ids= (dept-id), (store-id)

Table 8: HPO grid for DeepAR.

Hyperparameter	Search space
num_layers	[1, 2, 3, 4]
num_cells	[20, 30, 40, 50, 60, 70, 80, 90]
dropout_rate	[0.1, 0.2, 0.3, 0.4, 0.5]
cell_type	['lstm', 'gru']
context_length	[8, 16] for Tour [15, 25, 40, 60] for Wiki
num_epochs	[5, 10, 15, 20, 25, 30, 35, 40, 45, 50]
learning_rate	[0.0001, 0.001, 0.01]

Table 9: HPO grid for N-BEATS.

Hyperparameter	Search space
widths	[32, 64, 128, 256, 512]
meta_bagging_size	[5,10]
num_blocks	[1]
num_stacks	[1, 2, 5, 10, 15]
sharing	[True, False]
expansion_coefficient_	[16, 32]
lengths	[16, 32]
scale	[True, False]
epochs	[5,10,15,20,25,30,40,50]
learning_rate	[0.001]

Table 10: HPO grid for LightGBM (Tourism-L and Traffic Student Models)

Hyperparameter	Search space
colsample_bytree	[0.7, 0.5, 0.8, 1.0, 0.3, 0.4, 0.2]
learning_rate	[0.001, 0.1, 0.01]
max_bin	[10, 20, 30, 40, 50, 70, 100, 200]
min_child_samples	[10, 20, 30, 50, 100, 200, 400]
n_estimators	[500, 1000, 2000, 3000]
num_leaves	[10, 15, 31, 63, 127, 255]
subsample	[0.7, 0.5, 0.8, 1.0, 0.3, 0.4, 0.2]

Table 11: HPO grid for LightGBM M5 Teacher Model

Hyperparameter	Search space
colsample_bytree	[0.5, 0.7, 0.3]
learning_rate	[0.1, 0.01, 0.001]
max_bin	[10, 25, 50]
n_estimators	[200, 400, 600, 800, 1000, 2000]
num_leaves	[8, 16, 32, 64]
subsample	[0.7, 0.5, 0.3]
tweedie_variance_	[1, 1.1, 1.2, 1.3, 1.4, 1.5]
power	

Table 12: HPO grid for LightGBM M5 Student Model

Hyperparameter	Search space
learning_rate	[0.1, 0.015]
max_bin	[100, 200]
n_estimators	[2000, 3000]
num_leaves	[255, 128]
subsample	[0.3, 0.5]

Table 13: Level-wise RMSSE (mean±standard deviation) for the best H-PRO, best baseline, and best SOTA methods. The best score is in **bold**.

Dataset	Level	Ours	Best baseline	Best SOTA
Tourism	L1	0.3383±0.0156	0.6473±0.2636	0.3843±0.0249
	L2	0.4251±0.0129	0.7137±0.2408	0.4766±0.0072
	L3	0.5336±0.0065	0.6836±0.1222	0.5539±0.0123
	L4	0.5723±0.0062	0.6635±0.0902	0.5895±0.0116
Tourism-L	L1	0.1812±0.0066	0.1838±0.0106	0.1486±0.0000
	L2	0.3861±0.0083	0.3869±0.0083	0.4079±0.0000
	L3	0.4737±0.0004	0.4732±0.0032	0.4986±0.0000
	L4	0.5749±0.0010	0.5759±0.0017	0.5812±0.0000
	L5	0.4409±0.0077	0.4433±0.0080	0.4482±0.0000
	L6	0.5575±0.0004	0.5579±0.0047	0.5757±0.0000
	L7	0.6405±0.0033	0.6403±0.0045	0.6345±0.0000
	L8	0.6704±0.0036	0.6705±0.0039	0.6732±0.0000
Wiki	L1	0.1954±0.0329	0.3947±0.1591	0.1615±0.0000
	L2	0.3007±0.0180	0.4027±0.0846	0.3132±0.0000
	L3	0.3256±0.0151	0.3502±0.0390	0.3165±0.0000
	L4	0.4420±0.0152	0.4558±0.0321	0.5827±0.0000
	L5	0.3515±0.0042	0.3485±0.0108	0.5960±0.0000
Traffic	L1	0.1764±0.0070	0.2324±0.0124	0.2329±0.0058
	L2	0.2103±0.0106	0.2627±0.0139	0.2423±0.0108
	L3	0.2865±0.0154	0.3233±0.0071	0.2726±0.0155
	L4	0.8332±0.0168	0.7870±0.0155	0.8163±0.0547

Table 14: M5 results obtained via Department-wise clustering (Dept), Store-wise clustering (Store), and Ensemble of Dept. and Store cluster predictions (EDS). Hierarchical (R_H) and level-wise weighted RMSSE for H-Pro, Gold, M5 winning method (SOTA) and baseline (TCV-Hier) in M5 dataset are mentioned with standard deviation. The best and Gold score are in **bold**.

Cluster	Level	SOTA	Gold	Baseline	H-Pro-Top	H-Pro-Top PO	H-Pro-Avg	H-Pro-Avg PO
Dept	L1	0.199	0.175±0.007	0.222±0.003	0.175±0.007	0.188±0.002	0.223±0.003	0.223±0.005
	L2	0.31	0.288±0.007	0.328±0.002	0.288±0.007	0.304±0.003	0.327±0.003	0.328±0.006
	L3	0.4	0.397±0.005	0.437±0.002	0.397±0.005	0.409±0.002	0.433±0.002	0.432±0.005
	L4	0.277	0.229±0.004	0.273±0.005	0.229±0.004	0.250±0.006	0.274±0.003	0.274±0.005
	L5	0.365	0.317±0.006	0.349±0.004	0.317±0.006	0.336±0.002	0.349±0.004	0.355±0.011
	L6	0.39	0.367±0.007	0.406±0.003	0.367±0.007	0.386±0.004	0.403±0.003	0.406±0.006
	L7	0.474	0.450±0.003	0.480±0.002	0.450±0.003	0.468±0.004	0.478±0.003	0.485±0.009
	L8	0.48	0.473±0.003	0.512±0.003	0.473±0.003	0.489±0.003	0.508±0.002	0.509±0.005
	L9	0.573	0.566±0.000	0.595±0.001	0.566±0.000	0.580±0.004	0.591±0.002	0.596±0.006
	L10	0.966	1.028±0.004	1.010±0.002	1.028±0.004	1.033±0.001	1.012±0.001	1.017±0.002
	L11	0.929	0.976±0.003	0.959±0.002	0.976±0.003	0.979±0.001	0.960±0.000	0.965±0.001
	L12	0.884	0.919±0.001	0.906±0.001	0.919±0.001	0.922±0.001	0.907±0.000	0.911±0.001
	R_H	0.52	0.515±0.002	0.540±0.002	0.515±0.002	0.529±0.001	0.539±0.002	0.542±0.005
Store	L1	0.199	0.202±0.002	0.240±0.004	0.202±0.001	0.191±0.002	0.240±0.004	0.233±0.001
	L2	0.31	0.308±0.002	0.335±0.002	0.308±0.003	0.316±0.005	0.335±0.002	0.332±0.003
	L3	0.4	0.394±0.002	0.412±0.001	0.396±0.003	0.412±0.004	0.412±0.001	0.410±0.005
	L4	0.277	0.259±0.000	0.295±0.003	0.260±0.000	0.251±0.003	0.295±0.003	0.287±0.002
	L5	0.365	0.360±0.000	0.391±0.002	0.361±0.001	0.356±0.005	0.391±0.002	0.382±0.001
	L6	0.39	0.385±0.001	0.413±0.001	0.387±0.002	0.392±0.006	0.413±0.001	0.407±0.004
	L7	0.474	0.478±0.001	0.501±0.001	0.479±0.002	0.484±0.006	0.501±0.001	0.495±0.002
	L8	0.48	0.475±0.001	0.491±0.001	0.476±0.002	0.490±0.002	0.491±0.001	0.487±0.005
	L9	0.573	0.577±0.001	0.589±0.001	0.578±0.002	0.590±0.004	0.589±0.001	0.586±0.004
	L10	0.966	0.994±0.001	1.000±0.000	0.996±0.000	1.006±0.001	1.000±0.000	1.000±0.001
	L11	0.929	0.949±0.001	0.951±0.000	0.951±0.000	0.962±0.002	0.951±0.000	0.952±0.002
	L12	0.884	0.899±0.001	0.899±0.000	0.901±0.000	0.914±0.002	0.899±0.000	0.901±0.002
	R_H	0.52	0.523±0.001	0.543±0.001	0.524±0.001	0.530±0.003	0.543±0.001	0.539±0.002
EDS	L1	0.199	0.186±0.004	0.230±0.002	0.186±0.004	0.189±0.001	0.231±0.003	0.227±0.003
	L2	0.31	0.294±0.004	0.326±0.002	0.294±0.003	0.305±0.003	0.327±0.001	0.325±0.003
	L3	0.4	0.387±0.003	0.410±0.001	0.386±0.002	0.398±0.002	0.409±0.001	0.408±0.003
	L4	0.277	0.237±0.003	0.280±0.003	0.237±0.004	0.247±0.002	0.280±0.003	0.277±0.003
	L5	0.365	0.328±0.003	0.364±0.002	0.329±0.003	0.339±0.003	0.363±0.003	0.362±0.005
	L6	0.39	0.370±0.004	0.403±0.002	0.370±0.003	0.383±0.002	0.402±0.002	0.401±0.004
	L7	0.474	0.455±0.002	0.484±0.001	0.456±0.001	0.468±0.004	0.483±0.002	0.483±0.005
	L8	0.48	0.465±0.002	0.489±0.001	0.464±0.001	0.477±0.002	0.488±0.001	0.486±0.003
	L9	0.573	0.561±0.000	0.581±0.001	0.561±0.000	0.572±0.004	0.580±0.001	0.580±0.003
	L10	0.966	1.001±0.002	0.999±0.001	1.003±0.002	1.009±0.000	1.000±0.000	1.001±0.001
	L11	0.929	0.954±0.001	0.951±0.001	0.955±0.001	0.961±0.001	0.951±0.000	0.953±0.001
	L12	0.884	0.903±0.001	0.899±0.000	0.903±0.001	0.909±0.000	0.899±0.000	0.901±0.001
	R_H	0.52	0.512±0.001	0.535±0.001	0.512±0.001	0.521±0.002	0.534±0.001	0.534±0.003

 Table 15: Mean±Standard deviation of Hierarchical RMSSE, R_H of ensemble models with ids (1) to (4).

Data	(1)	(2)	(3)	(4)	SOTA	Baseline
Tourism	0.5058±0.0049	0.4789±0.0070	0.4831±0.0057	0.4865±0.0267	0.5011±0.0140	0.6770±0.1789
Tourism-L	0.4914±0.0020	0.4882±0.0007	0.4882±0.0007	0.4883±0.0008	0.4960±0.0000	0.4915±0.0020
Wiki	0.3229±0.0076	0.3229±0.0076	0.3229±0.0076	0.3523±0.0089	0.3940±0.0000	0.3904±0.0609
Traffic	0.3780±0.0135	0.3732±0.0110	0.3660±0.0044	0.3703±0.0058	0.3910±0.0217	0.4014±0.0073
M5	0.5202±0.0008	0.5199±0.0015	0.5186±0.0010	0.5210±0.0008	0.5200±0.0000	0.534±0.001